High Hydroxide Conductivity in Polymerized Ionic Liquid Block Copolymers

ARTICLE *in* ACS MACRO LETTERS · JUNE 2013

Impact Factor: 5.76 · DOI: 10.1021/mz400210a

5 AUTHORS, INCLUDING:

Eric M. Davis
Clemson University
16 PUBLICATIONS **81** CITATIONS
SEE PROFILE

Karen I Winey
University of Pennsylvania
331 PUBLICATIONS **11,304** CITATIONS
SEE PROFILE

ACS Macro Letters

Letter

pubs.acs.org/macroletters

High Hydroxide Conductivity in Polymerized Ionic Liquid Block Copolymers

Yuesheng Ye,[†,‡] Sharon Sharick,[†,§] Eric M. Davis,[‡] Karen I. Winey,*[,§] and Yossef A. Elabd*[,‡]

[‡]Department of Chemical and Biological Engineering, Drexel University, Philadelphia, Pennsylvania 19104, United States

[§]Department of Materials Science and Engineering, University of Pennsylvania, Philadelphia, Pennsylvania 19104, United States

Supporting Information

ABSTRACT: Herein, we report a polymerized ionic liquid diblock copolymer with high hydroxide conductivity and nanoscale morphology. Surprisingly, the conductivity is not only higher (over an order of magnitude) than its random copolymer analog at the same ion and water content, but also higher than its homopolymer analog, which has a higher ion and water content than the block copolymer. These results should have a significant impact on low-cost (platinum-free), long-lasting, solid-state alkaline fuel cells.

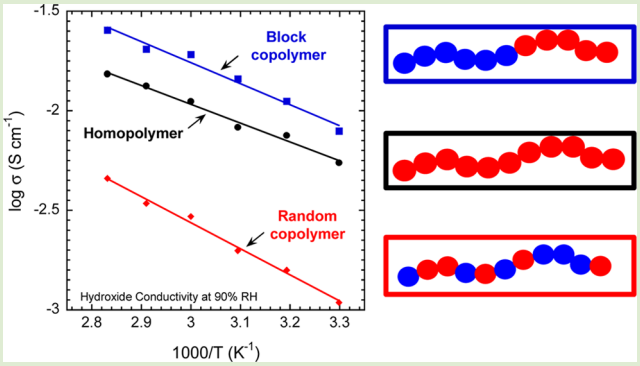

Solid-state alkaline fuel cells (AFCs), utilizing anion exchange membranes (AEMs) as electrolytes rather than caustic alkaline liquid electrolytes, have recently attracted significant attention due to their potential to produce high power densities with long lifetimes at a lower cost (platinum-free) compared to traditional proton exchange membrane (PEM) fuel cells.[1−5] However, the chemical stability of ammonium-based AEMs (most commonly reported AEM chemistry) in dry and alkaline conditions is a major limiting factor for the development of long-lasting solid-state AFCs.[1,6,7] A broader variety of AEM chemistries have recently been reported to address this issue.[8−11] In 2011, a study by Ye and Elabd[12] showed enhanced chemical stability over a wide range of humidities and temperatures for a hydroxide (OH^-)-exchanged imidazolium-based polymerized ionic liquid (PIL), which was attributed to the delocalization of the imidazolium cation charge through the conjugated structure,[13] relatively stable *N*-heterocyclic carbene structure under dry conditions,[14] and imidazolium-carbene reversibility under wet−dry cycling.[13] The enhanced chemical stability of the imidazolium cation has attracted interest in the development of imidazolium-based AEMs. For example, a number of recent investigations report on the synthesis and characterization of hydroxide-conducting imidazolium-based PIL random copolymers.[15−19] However, there are few reports of hydroxide-conducting imidazolium-based PIL block copolymers.[20]

In contrast, proton-conducting block copolymers have been extensively investigated, where a number of studies have shown enhanced conductivity in block copolymers compared to their random copolymer analogs due to their well-defined nanostructured morphologies.[21−26] Indeed, several hydroxide-conducting ammonium-based block copolymers have recently been reported in the literature.[27−31] However, there is limited information regarding their morphologies and more importantly their ion transport−morphology relationships. More in-depth investigations that can provide a fundamental understanding of hydroxide transport in chemically stable hydroxide-conducting block copolymers would be of significant interest.

In this paper, we report the high hydroxide conductivity of a chemically stable imidazolium-based PIL diblock copolymer. The conductivity is over an order of magnitude higher than its PIL random copolymer analog at the same ion and water content. More surprisingly, the conductivity is higher than its PIL homopolymer analog, where the homopolymer has a higher ion and water content than the block copolymer. The morphologies and states of water in these polymers were characterized with transmission electron microscopy (TEM), in situ small-angle X-ray scattering (SAXS), and in situ Fourier transform infrared, attenuated total reflectance (FTIR-ATR) spectroscopy to provide a deeper understanding of hydroxide ion transport in nanostructured polymers.

The hydroxide-exchanged PIL diblock copolymer, poly(MMA-*b*-MEBIm-OH), comprised of an ionic liquid (IL) component (1-[(2-methacryloyloxy)ethyl]-3-butylimidazolium hydroxide, MEBIm-OH) and a nonionic component (methyl methacrylate, MMA), was synthesized via anion exchange metathesis from its precursor bromide (Br^-)-exchanged PIL diblock copolymer, poly(MMA-*b*-MEBIm-Br) (see Supporting Information). For comparison, a random copolymer analog, at the same IL composition or ion exchange capacity (IEC), and

Received: April 28, 2013
Accepted: June 6, 2013
Published: June 11, 2013

   dx.doi.org/10.1021/mz400210a | *ACS Macro Lett.* 2013, 2, 575−580

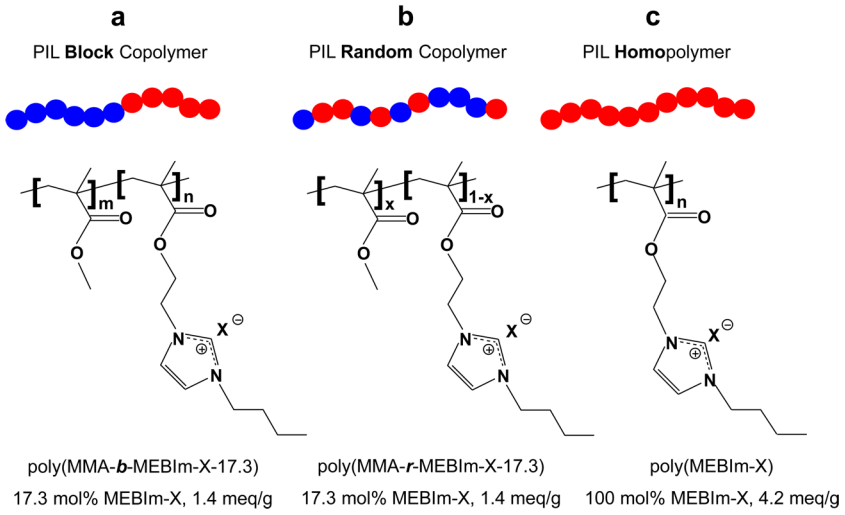

Figure 1. Polymer chain architecture (blue and red correspond to MMA and MEBIm-X, respectively), chemical structure, and ion exchange capacity (IEC) of (a) PIL block copolymer: poly(MMA-*b*-MEBIm-X-17.3), (b) PIL random copolymer: poly(MMA-*r*-MEBIm-X-17.3), and (c) PIL homopolymer: poly(MEBIm-X). X corresponds to the counteranion, which is either bromide (Br^-) or hydroxide (OH^-). The block and random copolymers have 17.3 mol % of the IL component (MEBIm-X), which corresponds to an IEC of 1.4 meq Im^+ g^{-1} polymer. The homopolymer has 100 mol % MEBIm-X corresponding to 4.2 meq g^{-1}.

the PIL homopolymer analog were synthesized (Figure 1). The physical properties of these PIL polymers are listed in the Supporting Information (Table S1) and a detailed description of the synthesis of the precursor polymers have been described elsewhere.[12,32]

We first present the bromide ion conductivity of the block and random copolymers at the same IL (MEBIm-Br) composition (17.3 mol %) or IEC (1.4 meq g^{-1}) and the subsequent block copolymer morphology over a range of humidities and temperatures (Figure 2). Figure 2b shows the bromide conductivity at 30 °C as a function of relative humidity (RH) from 30 to 90% RH for the block and random copolymers (both 1.4 meq g^{-1}) and the PIL homopolymer (4.2 meq g^{-1}). As expected, the bromide conductivity increases over 3 orders of magnitude with increasing RH for all polymers. This can be attributed to a water-assisted transport mechanism, where an increase in polymer water content (3 to 34 wt %) and corresponding hydration number (λ = 1−8 mol water/mol Im^+; see Supporting Information, Figure S2) were observed over this humidity range for all polymers. This transport mechanism is similar to water−Nafion systems,[33] where proton transport is dictated by a water-assisted process, but differs from lithium salt−poly(ethylene oxide) systems,[34] where lithium ion transport in an anhydrous polymer is dictated by the segmental dynamics of the polymer chains.

Interestingly, the bromide conductivities of the block copolymer are 1−2 orders of magnitude higher than the random copolymer with this difference decreasing with increasing humidity. It is important to note that the water content in the block and random copolymer are identical at each relative humidity (see Supporting Information, Figure S2). Therefore, both the IEC and water content are similar in these copolymers, but the bromide conductivity is significantly different, where the only difference between the block and the random copolymers is the polymer chain architecture (see Figure 1), which results in differences in morphology. Surprisingly, the bromide conductivity of the block copolymer is higher than the homopolymer at 90% RH and 30 °C, 1.12 versus 0.87 mS cm^{-1}, respectively, while the IEC and water contents are higher in the homopolymer, 1.4 versus 4.2 meq g^{-1} and 18 versus 34 wt % for the block copolymer and homopolymer, respectively (see Supporting Information, Figure S2).

Figure 2c shows bromide conductivity at 90% RH as a function of temperature from 30 to 80 °C for all polymers. The block copolymer bromide conductivity increases from 1.12 to 5.67 mS cm^{-1} with increasing temperature. This is higher than both the random copolymer and the homopolymer at all temperatures. Note that the IEC and water content of the block and random copolymers are also identical over this temperature range, while the IEC and water content in the homopolymer are higher than the block copolymer (see Supporting Information, Figure S2). The bromide conductivity in all polymers follows an Arrhenius behavior with temperature at high humidity with activation energies of 29, 31, and 25 kJ mol^{-1} for the block copolymer, random copolymer, and homopolymer, respectively.

To provide deeper insight into these unusual ion conductivity results, the morphologies of the block and random copolymers were examined by in situ small-angle X-ray scattering (SAXS) at humidified conditions in an environmental chamber[35] and with transmission electron microscopy (TEM). As expected, the SAXS profile for the random copolymer was featureless indicating no microphase separation (see Supporting Information, Figure S6). Figure 2e,f shows SAXS profiles of the block copolymer at various humidities and temperatures. At 30 °C, in both dry and low relative humidity (30% RH) conditions, there are four well-defined scattering peaks with positions q^* (primary peak), $2q^*$, $3q^*$, and $4q^*$, indicative of strongly microphase-separated lamellar morphology with long-range order. The TEM image of the block copolymer under dry conditions (Figure 2d) confirms this morphology assignment. As humidity increases to 60% RH, the second and fourth correlation peaks in the SAXS profiles decrease in intensity and are no longer visible at 90% RH. The absence of the expected peaks at $2q^*$ and $4q^*$ at 90% RH is consistent with having approximately equal volume fractions of the dry MMA and hydrated IL microphases (see Supporting

dx.doi.org/10.1021/mz400210a | *ACS Macro Lett.* 2013, 2, 575−580

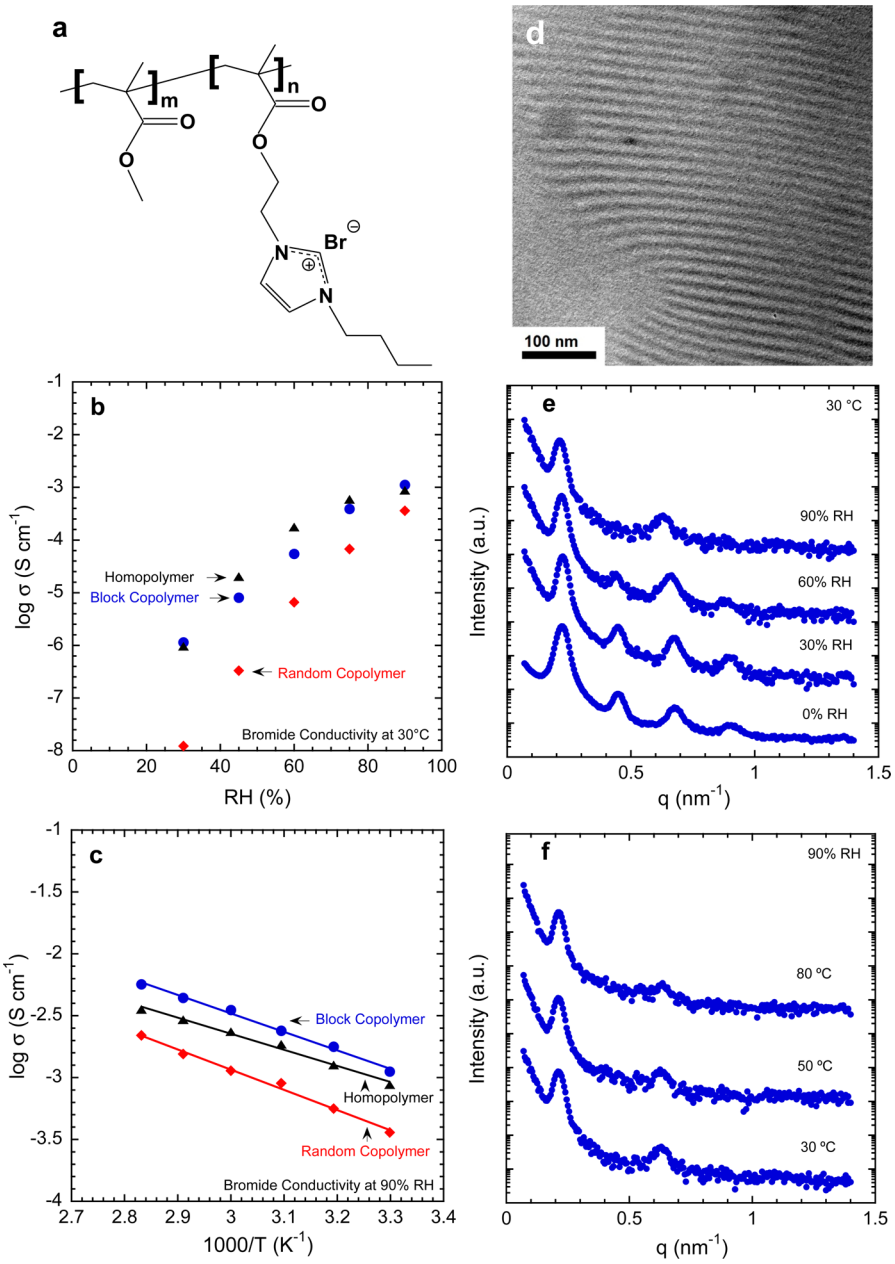

Figure 2. (a) Chemical structure of bromide-conducting PIL copolymer. Bromide conductivity as a function of (b) humidity at 30 °C and (c) temperature at 90% RH for the PIL block copolymer poly(MMA-*b*-MEBIm-Br-17.3) (blue circles), random copolymer poly(MMA-*r*-MEBIm-Br-17.3) (red diamonds), and homopolymer poly(MEBIm-Br), (black triangles). (d) Transmission electron microscopy image of PIL block copolymer at room temperature under vacuum. Sample unstained; dark regions correspond to IL (MEBIm-Br) microdomains. SAXS profiles of the PIL block copolymer as a function of (e) humidity at 30 °C and (f) temperature at 90% RH. The lamellae period, a_{lam}, ranged from 27.8 to 29.9 nm and the IL microdomain thickness, l_{IL}, ranged from 11.1 to 14.9 nm over all temperature and humidity conditions. SAXS data were collected in an environmental chamber and data are offset vertically for clarity.

Information) and minima in the scattering form factor at $2q^*$ and $4q^*$. With regard to the scattering as a function of temperature at 90% RH, the change is negligible (Figure 2f). It should also be noted that the changes in scattering as a function of humidity and temperature are reversible (see Supporting Information, Figure S7). This study indicates that under different humidified conditions the lamellar morphology persists. In addition to the morphological differences between block and random copolymers (microphase-separated lamellar morphology versus no microphase separation), in situ time-resolved FTIR-ATR spectroscopy was employed to investigate the water structure in the polymers, where a higher distribution of water clusters was observed in the block copolymer compared to the random copolymer suggesting differences in ion transport mechanisms (see Supporting Information, Figure S8).

Figure 3 shows the hydroxide ion conductivity of the block and random copolymer at the same IL composition and the subsequent block copolymer morphology over a range of humidities and temperatures. The hydroxide conductivity trends (Figure 3b,c) are similar to the bromide conductivity data (Figure 2b,c) with the primary difference in the overall higher magnitude in ion conductivity. For example, the hydroxide and bromide conductivity in the block copolymer

dx.doi.org/10.1021/mz400210a | *ACS Macro Lett.* 2013, 2, 575−580

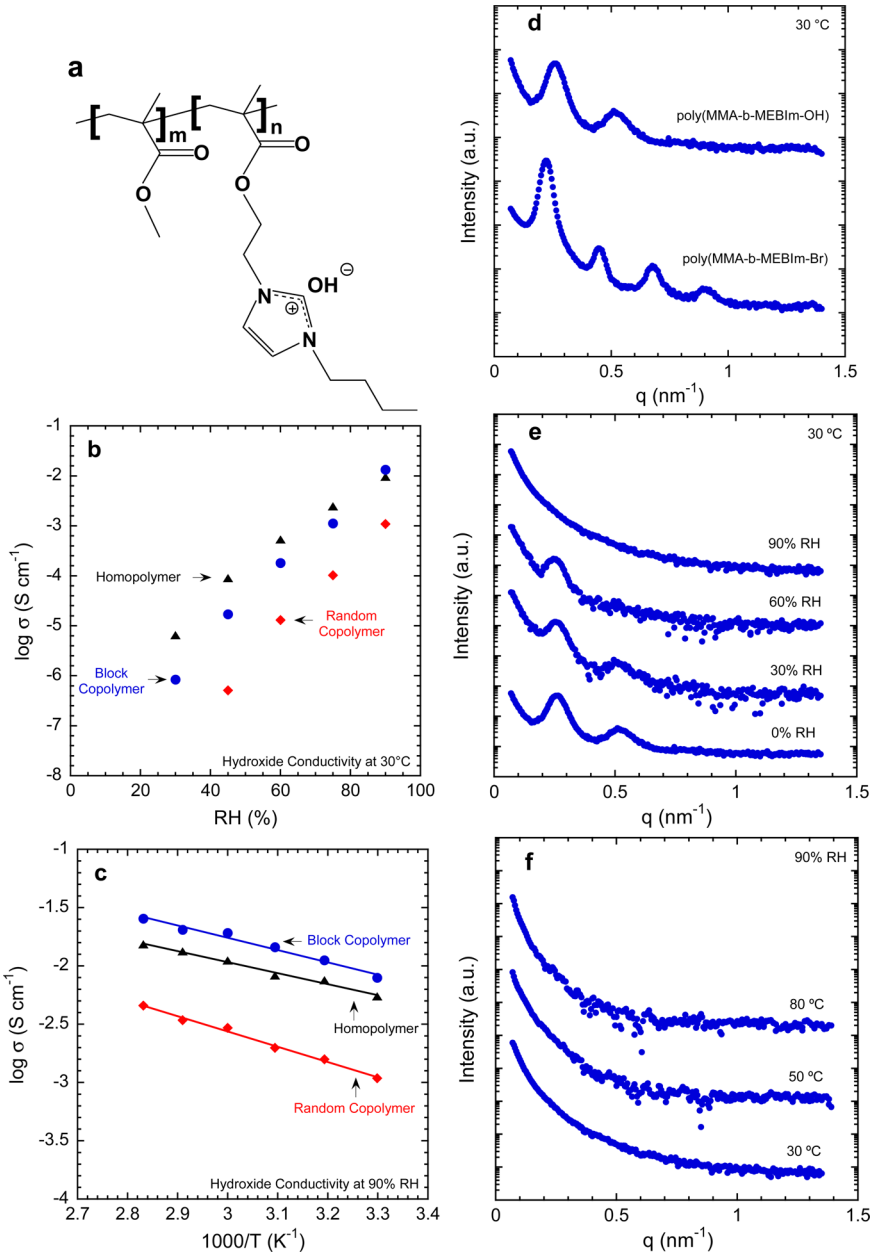

Figure 3. (a) Chemical structure of hydroxide-conducting PIL copolymer. Hydroxide conductivity as a function of (b) humidity at 30 °C and (c) temperature at 90% RH for the PIL block copolymer, poly(MMA-*b*-MEBIm-OH-17.3) (blue circles), random copolymer poly(MMA-*r*-MEBIm-OH-17.3) (red diamonds), and homopolymer poly(MEBIm-OH) (black triangles). SAXS profiles of the (d) bromide (poly(MMA-*b*-MEBIm-Br-17.3) vs the hydroxide (poly(MMA-*b*-MEBIm-OH-17.3) conducting PIL block copolymers at 0% RH and 30 °C. SAXS profiles of hydroxide-conducting block copolymer as a function of (e) humidity at 30 °C and (f) temperature at 90% RH. The lamellae period, a_{lam}, ranged from 24.1 to 25.1 nm and the IL microdomain thickness, l_{IL}, ranged from 9.3 to 10.4 nm over all temperature and humidity conditions. SAXS data were collected in an environmental chamber and data are offset vertically for clarity.

at 90% RH and 30 °C are 7.91 and 1.12 mS cm^{-1}, respectively, which corresponds to ca. 7-fold difference. Sudre et al.[20] recently reported ca. 10-fold difference between hydroxide and chloride conductivity in a block copolymer. A similar 7-fold difference in conductivity is apparent in the homopolymer, while the conductivity difference in the random copolymer is ca. 3-fold. Interestingly, the difference in the infinite dilution (in aqueous solution at 25 °C) conductivity or diffusivity between hydroxide and bromide is ca. 2.5-fold (OH^- = 0.0198 m^2 S mol^{-1}, 5.273 × 10^{-5} cm^2 s^{-1}; Br^- = 0.00781 m^2 S mol^{-1}, 2.080 × 10^{-5} cm^2 s^{-1}).[36] In addition to the infrared results, these results further suggest differences in the ion transport mechanisms in the block copolymer compared to the random copolymer.

Similar to the bromide conductivity results, the hydroxide conductivities of the block copolymer are an order of magnitude (range of 33- to 5-fold) higher than the random copolymer at all humidities and temperatures (Figure 3b,c). Similarly, the water content in the hydroxide-conducting block and random copolymer are identical at each humidity and temperature studied (see Supporting Information, Figure S3). Again, the IEC, water content, and chemical structure are similar in both block and random copolymer with the only difference being the sequential order of the monomer units in

dx.doi.org/10.1021/mz400210a | *ACS Macro Lett.* 2013, 2, 575−580

the polymer chain (i.e., chain architecture). While this difference in ion conductivity between block and random copolymers has been observed before in the literature in regards to water-assisted proton transport,[21] we report this result for hydroxide conductivity for the first time to our knowledge.

The more surprising result is that the hydroxide conductivity of the block copolymer is higher (~50%) than the homopolymer at 90% RH at all temperatures studied: 7.91 versus 5.48 mS cm^{-1} (at 30 °C, 90% RH) and 25.46 versus 15.29 mS cm^{-1} (at 80 °C, 90% RH), respectively. Again, note that the IEC and water contents of these two polymers are significantly different: 1.4 versus 4.2 meq g^{-1} and 19 versus 61 wt % (at 30 °C, 90% RH) for the block copolymer and homopolymer, respectively (see Supporting Information, Figure S3). However, their normalized water contents (i.e., hydration numbers) are relatively similar, ca. 8 mol water/mol Im^+ at all humidities and temperatures studied. Therefore, this result is unusual and suggests that other factors may result in higher transport in the block copolymer compared to the homopolymer, that is, ion−water confinement in nanochannels that may accelerate transport. To the authors' knowledge, this result of water-assisted ion transport higher in a block copolymer compared to its homopolymer analog has not been previously reported. This result compares to a recent report demonstrating enhanced ionic liquid-assisted proton conductivity in a block copolymer compared to its homopolymer analog in anhydrous conditions.[37]

Higher hydroxide conductivities in other anion exchange membranes have been reported,[3] but these are usually at higher IECs or much higher water contents. The hydroxide conductivity in this PIL block copolymer is quite high for such low water contents (ca. 8 mol water/mol Im^+). It is also interesting to compare the absolute magnitude of hydroxide conductivity in these block copolymers to proton conductivity in Nafion (the most widely cited proton-conducting polymer):[33] 7.91 versus 78.5 mS cm^{-1}[38] (at 30 °C, 90% RH) and 25.46 versus 144.00 mS cm^{-1}[38] (at 80 °C, 90% RH), respectively. The infinite dilution (in aqueous solution at 25 °C) conductivity or diffusivity of hydroxide is ca. 57% of that of protons (OH^- = 0.0198 m^2 S mol^{-1}, 5.273 × 10^{-5} cm^2 s^{-1}; H^+ = 0.034965 m^2 S mol^{-1}, 9.311 × 10^{-5} cm^2 s^{-1}),[36] while the hydroxide conductivity in the PIL block copolymer in this study is 10 and 20% at 30 and 80 °C, respectively, of that of proton conductivity in Nafion. Similar to proton conductivity in Nafion, the hydroxide conductivity in these PIL polymers follows an Arrhenius behavior with temperature at high humidity (Figure 3c) with activation energies of 20, 25, and 18 kJ mol^{-1} for the block copolymer, random copolymer, and homopolymer, respectively. These activation energies are lower than that of bromide conductivity in these PIL polymers, but higher than that for proton conductivity in Nafion (~11 kJ mol^{-1}).[38]

Morphologies in the hydroxide-exchanged PIL polymers were also investigated. SAXS profiles as a function of humidity and temperature for the hydroxide-conducting block copolymer are shown in Figure 3. Similar to the bromide-conducting random copolymer, the SAXS profile of the hydroxide-conducting random copolymer was featureless, indicating no microphase separation (see Supporting Information, Figure S6). Figure 3d compares the SAXS profiles of the hydroxide- and bromide-conducting block copolymers at a dry condition. Unlike the bromide-conducting block copolymer, where four well-defined scattering peaks were observed in the SAXS profile, the hydroxide-conducting block copolymer shows two broader scattering peaks at positions of q^* (primary peak) and $2q^*$, suggesting a weaker microphase separation. This was also observed at 30% RH (30 °C), but as humidity increases to 60% RH, only the primary peak was observed (Figure 3e). At 90% RH, the SAXS profiles are featureless for all investigated temperatures (Figure 3e,f). This morphology transformation is reversible (see Supporting Information, Figure S7).

One possible reason for the absence of these features in the SAXS profile in the block copolymer at high humidity is low electron density contrast between the MMA and hydrated IL microdomains. Further evidence for a loss of scattering contrast is the absence a correlation peak at high humidity, because block copolymers with sufficient contrast exhibit a correlation peak even in the disordered state. These results suggest that the nanoscale morphology in the hydroxide-conducting block copolymer persists at higher humidities similar to the bromide-conducting block copolymer (although not evidenced in the SAXS data) providing a rationale for the high hydroxide conductivities in comparison to the random copolymer. Note also that the macroscopic shape of the polymer film is retained when exposed to high relative humidity, which is also consistent with maintaining an ordered state.

Note that the hydroxide form in the PIL block copolymer was obtained via anion exchange with the bromide form in an alkaline solution. Therefore the Br^- ions are displaced by smaller OH^- ions in the solid-state film. Additionally, unlike the bromide-conducting block copolymer film, the hydroxide-conducting PIL block copolymer film was not annealed at a high temperature after ion exchange to circumvent any possible chemical degradation of the polymer.[12] These factors may contribute to a more poorly defined morphology compared to the bromide-conducting block copolymer. However, despite the difference in morphology, both PIL block copolymers exhibited superior ionic conductivities, particularly over their random copolymer and homopolymer analogs.

In summary, we report high hydroxide conductivity in a PIL block copolymer, for example, 25 mS cm^{-1} at 80 °C, 90% RH with only ca. 8 mol water/mol Im^+. The hydroxide conductivity is over an order of magnitude higher than its PIL random copolymer analog at the same IEC and water content. More surprisingly, we observed higher conductivity in the PIL block copolymer (with just 37 vol% PIL) compared to its PIL homopolymer analog, where the homopolymer has a significantly higher IEC and water content. The PIL block copolymer exhibits nanoscale morphology, while the PIL random copolymer exhibits no microphase separation. This nanoscale morphology may contribute to significantly different transport mechanisms, that is, ion−water confinement in nanochannels that accelerate transport. These results should have a significant impact on low-cost (platinum-free) long-lasting solid-state alkaline fuel cells.

■ ASSOCIATED CONTENT

Supporting Information

Materials, synthesis, experimental procedures, polymer water content data, supporting small-angle X-ray scattering data, and Fourier transform infrared-attenuated total reflectance spectroscopy data. This material is available free of charge via the Internet at http://pubs.acs.org.

AUTHOR INFORMATION

Corresponding Author

*E-mail: elabd@drexel.edu; winey@seas.upenn.edu.

Author Contributions

†These authors contributed equally.

Notes

The authors declare no competing financial interest.

ACKNOWLEDGMENTS

The authors gratefully acknowledge the U.S. Army Research Office for the financial support (Grant W911NF-07-1 0452, Ionic Liquids in Electro-Active Devices (ILEAD) MURI), as well as the Laboratory for Research on the Structure of Matter at Penn (MRSEC NSF DMR11-20901) for instrument support.

REFERENCES

(1) Varcoe, J. R.; Slade, R. C. T. *Fuel Cells* **2005**, *5*, 187−200.
(2) Couture, G.; Alaaeddine, A.; Boschet, F.; Ameduri, B. *Prog. Polym. Sci.* **2011**, *36*, 1521−1557.
(3) Merle, G.; Wessling, M.; Nijmeijer, K. *J. Membr. Sci.* **2011**, *377*, 1−35.
(4) Zhang, H. W.; Zhou, Z. T. *Prog. Chem.* **2008**, *20*, 602−619.
(5) Pan, J.; Chen, C.; Zhuang, L.; Lu, J. *Acc. Chem. Res.* **2012**, *45*, 473−481.
(6) Chempath, S.; Einsla, B. R.; Pratt, L. R.; Macomber, C. S.; Boncella, J. M.; Rau, J. A.; Pivovar, B. S. *J. Phys. Chem. C* **2008**, *112*, 3179−3182.
(7) Ye, Y.; Elabd, Y. A. In Polymers for Energy Storage and Delivery: Polyelectrolytes for Batteries and Fuel Cells. ACS Symposium Series 1096; Page, K. A., Soles, C. L., Runt, J., Eds.; Oxford University Press: New York, 2012; pp 234−251.
(8) Gu, S.; Cai, R.; Luo, T.; Chen, Z.; Sun, M.; Liu, Y.; Yan, Y. *Angew. Chem., Int. Ed.* **2009**, *48*, 6499−6502.
(9) Thomas, O. D.; Soo, K. J. W. Y.; Peckham, T. J.; Kulkarni, M. P.; Holdcroft, S. *J. Am. Chem. Soc.* **2012**, *134*, 10753−10756.
(10) Zhang, B.; Gu, S.; Wang, J.; Liu, Y.; Herring, A. M.; Yan, Y. *RSC Adv.* **2012**, *2*, 12683−12685.
(11) Noonan, K. J. T.; Hugar, K. M.; Kostalik, H. A., IV; Lobkaovsky, E. B.; Abruña, H. D.; Coates, G. W. *J. Am. Chem. Soc.* **2012**, *134*, 18161−18164.
(12) Ye, Y.; Elabd, Y. A. *Macromolecules* **2011**, *44*, 8494−8503.
(13) Amyes, T. L.; Diver, S. T.; Richard, J. P.; Rivas, F. M.; Toth, K. *J. Am. Chem. Soc.* **2004**, *126*, 4366−4374.
(14) Wolfgang, A.; Herrmann, W. A.; Köcher, C. *Chem. Int. Ed.* **1997**, *36*, 2162−2187.
(15) Guo, M.; Fang, J.; Xu, H.; Li, W.; Lu, X.; Lan, C.; Li, K. *J. Membr. Sci.* **2010**, *362*, 97−104.
(16) Lin, B.; Qiu, L.; Lu, J.; Yan, F. *Chem. Mater.* **2010**, *22*, 6718−6725.
(17) Lin, B.; Qiu, L.; Qiu, B.; Peng, Y.; Yan, F. *Macromolecules* **2011**, *44*, 9642−9649.
(18) Zhang, F.; Zhang, H.; Qu, C. *J. Mater. Chem.* **2011**, *21*, 12744−12752.
(19) Yan, X.; He, G.; Gu, S.; Wu, X.; Du, L.; Wang, Y. *Int. J. Hydrogen Energy* **2012**, *37*, 5216−5224.
(20) Sudre, G.; Inceoglu, S.; Cotanda, P.; Balsara, N. P. *Macromolecules* **2013**, *46*, 1519−1527.
(21) Elabd, Y. A.; Hickner, M. A. *Macromolecules* **2011**, *44*, 1−11.
(22) Shi, Z. Q.; Holdcroft, S. *Macromolecules* **2005**, *38*, 4193−4201.
(23) Roy, A.; Hickner, M. A.; Yu, X.; Li, Y.; Glass, T. E.; McGrath, J. E. *J. Polym. Sci., Polym. Phys.* **2006**, *44*, 2226−2239.
(24) Elabd, Y. A.; Napadensky, E.; Walker, C. W.; Winey, K. I. *Macromolecules* **2006**, *39*, 399−407.
(25) Bae, B.; Miyatake, K.; Watanabe, M. *ACS Appl. Mater. Int.* **2009**, *1*, 1279−1286.
(26) Roy, A.; Yu, X.; Dunn, S.; McGrath, J. E. *J. Membr. Sci.* **2009**, *327*, 118−124.
(27) Zeng, Q. H.; Liu, Q. L.; Broadwell, I.; Zhu, A. M.; Xiong, Y.; Tu, X. P. *J. Membr. Sci.* **2010**, *349*, 237−243.
(28) Lee, K. M.; Wycisk, R.; Litt, M.; Pintauro, P. N. *J. Membr. Sci.* **2011**, *383*, 254−261.
(29) Zhao, Z.; Wang, J.; Li, S.; Zhang, S. *J. Power Sources* **2011**, *196*, 4445−4450.
(30) Tanaka, M.; Fukasawa, K.; Nishino, E.; Yamaguchi, S.; Yamada, K.; Tanaka, H.; Bae, H.; Miyatake, K.; Watanabe, M. *J. Am. Chem. Soc.* **2011**, *133*, 10646−10654.
(31) Disabb-Miller, M. L.; Johnson, Z. D.; Hickner, M. A. *Macromolecules* **2013**, *46*, 949−956.
(32) Ye, Y.; Choi, J.-H.; Winey, K. I.; Elabd, Y. A. *Macromolecules* **2012**, *45*, 7027−7035.
(33) Mauritz, K. A.; Moore, R. B. *Chem. Rev.* **2004**, *104*, 4535−4585.
(34) Ratner, M. A.; Shriver, D. F. *Chem. Rev.* **1988**, *88*, 109−124.
(35) Salas-de la Cruz, D.; Denis, J. G.; Griffith, M. D.; King, D. R.; Heiney, P. A.; Winey, K. I. *Rev. Sci. Instrum.* **2012**, *83*, 025112.
(36) *CRC Handbook of Chemistry and Physics*, 74th ed.; Lide, D. R., Ed.; CRC Press: Boca Raton, FL, 1993.
(37) Kim, S. Y.; Kim, S.; Park, M. J. *Nat. Commun.* **2010**, *88*, 1−7.
(38) Chen, L.; Hallinan, D. T., Jr.; Elabd, Y. A.; Hillmyer, M. A. *Macromolecules* **2009**, *42*, 6075−6085.